A Data-Driven Dynamic Model and Model Reference Control of Inverter Based Resources

Ganesh Marasini[1,3], Kenneth McDonald[1,3], Zhihua Qu[2,3,5], Thomas E. McDermott[2,4]

***Abstract*—Accurate and computationally tractable models of inverter based resources (IBRs) are necessary for control design and performance evaluations of these devices in the present grid. This paper discusses the data-driven approach to obtain the non-linear data-driven model. Specifically, a Hammerstein Wiener (HW) model of a three-phase inverter is obtained using the open-source *dynoNet* application to obtain the parameters of the model. To demonstrate the application of the model, a model reference control (MRC) strategy is proposed for the inverter to achieve the grid-forming objective of reference voltage tracking. The high fidelity simulation results from the test in MATLAB/SIMULINK environment demonstrate the good performance of the HW model and its efficacy in tracking the reference voltage through MRC strategy.**

I. Introduction

The usage of power electronic devices such as DC/DC converters and DC/AC inverters for the integration of renewable energy resources in the smart grid is ever increasing, due to their flexibility in implementing the associated control algorithms [1]. For successful and efficient integration of these control algorithms, it is essential to analyze the effects of power electronic technologies on the performance and stability of the grid, since the operating principle of these devices are different from that of the conventional synchronous generators. It is also important to ensure that the controllers designed for these devices contribute to the overall system stability by correctly meeting operational objectives.

To properly design robust control for, and conduct comprehensive system analysis involving power electronic devices, it is crucial to develop an accurate and computationally tractable model. An accurate model should be able to capture the dynamics related to the on/off operation modes of PWM switches, as well as the effects of passive elements such as inductors, capacitors, and resistors. Additionally, the model should account for the influence of various control elements, including dead-bands and saturation techniques.

The most accurate modeling approach is to explicitly consider the behavior of the device during each on/off operating modes of the PWM switches [2], where the dynamics of the passive elements are typically represented through state equations or transfer functions. Such a detailed model is able to capture all the switching dynamics accurately. However, it is computationally demanding to use in simulation studies and mathematically complex to use in the controller design. Another approach is the averaged switch modeling technique [3]. The basic assumption is made that the natural time constants of the converter are much longer than the switching period, so that the converter contains low-pass filtering of the switching harmonics. One may average the waveforms over an interval that is short compared to the system natural time constants, without significantly altering the system response. In particular, averaging over the switching period removes the switching harmonics, while preserving the low-frequency components of the waveforms. This step removes the small but mathematically-complicated switching harmonics, leading to a relatively simple and tractable converter model.

Of the more recent approaches, the data-driven approach stands out. In contrast to the previously described approaches that rely on the physical properties of the system to derive the model, the data-driven approach exploits the simulated or experimental input-output data to facilitate the development of a model, either linear or non-linear, that accurately reflect the dynamics of the system. The linear model is typically represented by a simple transfer function or state-space system. For a nonlinear system, the linear model can be preceded and followed by a nonlinearity consisting of linear transformations and nonlinear activation functions to create a Hammerstein-Weiner (HW) model.

Once the structure of the desired model has been determined, various system identification and machine learning methods can be utilized to identify and tune the model parameters. In [4], [5], transfer function models are obtained for commercial off-the-shelves inverter. A power hardware-in-the-loop (PHIL) test system consisting of a commercial inverter connected to a grid simulator was used to collect the required data and the model parameters were obtained using the MATLAB's system identification toolbox. However, the linear models cannot capture the non-linear dynamics of the system and as a workaround the non-linear dynamics can be piecewise linearized, and a linear model can be obtained for each linearized region. In [6], HW modeling for a single-phase grid connected photovoltaic inverter has been discussed. A three-phase inverter system has many complexities such as reference frame transformations, coupling between axes, etc. These complexities are not present in the single-phase inverter system. Since, the use of three-phase inverter is ubiquitous in today's grid, it is relevant to explore the non-linear modeling capabilities for such inverters.

Our companion paper [7] discusses the HW model alternatives, architecture, training, validation, and stability. It de-

1:Student, IEEE; 2: Fellow, IEEE; 3:Department of Electrical and Computer Engineering, University of Central Florida, Orlando, FL 32816, USA; 4: Meltran, Charlottesville, VA 22901-9053; 5: Corresponding author (email: qu@ucf.edu). This work was supported by the U.S. Department of Energy under Award DE-EE0009028.

scribes other use cases for continuous time domain, integration with electromagnetic transient (EMT) simulators, and model portability. The HW model is trained with the AC output filter included, which improves accuracy and guarantees that training data are accessible at the inverter's AC terminals. This paper builds on the work in [7] by removing AC output filter effects from the HW model, which is necessary for the use case of real-time control. We then demonstrate use of the compensated model to improve control performance in tracking the reference voltage.

The rest of the paper is organized as follows: section II introduces the test system and presents the average modeling and HW modeling approach for the test system. Section III presents the details on HW modeling of the test system, the MRC for the test system to achieve reference voltage tracking is presented in section IV. Section V presents and discusses the results, and section VI concludes the paper.

II. Test System and IBR Models

Fig. 1 shows the circuit diagram of the test system considered in this work. The test system consists of PV array, DC/DC boost converter with its controller (not shown in Fig. 1), DC-link capacitor, a three-level neutral point clamped (NPC) inverter with LC filter at its output terminals which are connected to local loads. Fig. 2 shows the simplified single line diagram of the test system; the DC-stage is simplified as a controllable voltage source. For a given weather condition, the DC-link voltage is regulated by the controller (not shown in these figures) for the boost converter. R_f, L_f, and C_f are the resistance, inductance and capacitance of the LC filter. The measurement variables i_s, v_o, i_o, and V_{DC} are the inductor current, output voltage, output current, and DC voltage respectively. The control variables u_c and ω_c are the modulation index for the PWM operation and control frequency respectively. The variable v_s is the fundamental component of the voltage at the PWM terminal of the inverter.

Ideally, the detailed model of Fig. 1, which represents the inverter dynamics through switching stages of PWM switches and differential equations of LCL filter, is the closest representation of the inverter hardware. However, such a model is not computationally tractable for real-time control and is not in the suitable form to be used in the controller design process. As an alternative, other models are used which are described below:

A. Average Model

The simplified dynamic model of the inverter, in synchronous reference frame, is given as:

$$v_s^{avg} = \frac{v_{dc}}{2} u_c, \quad \dot{\delta}_o = \omega - \omega_0, \quad \omega = \omega_c, \tag{1}$$

where δ_o is the phase angle of v_o. The LCL filter has the following vector-form state-space model:

$$\frac{dv_o}{dt} = A_{21} i_o + A_{22} v_o + A_{23} i_s \tag{2}$$

$$\frac{di_s}{dt} = A_{32} v_o + A_{33} i_s + B_3 u, \tag{3}$$

where $i_s = [i_{sd} \quad i_{sq}]^\top$, $v_o = [v_{od} \; v_{oq}]^\top$, $i_o = [i_{od} \; i_{oq}]^\top$, $u_c = [u_{cd} \; u_{cq}]^\top$,

$$A_{21} = -\frac{1}{C_f} I_{2\times 2}, \qquad A_{22} = \begin{bmatrix} 0 & \omega_c \\ -\omega_c & 0 \end{bmatrix},$$

$$A_{32} = -\frac{1}{L_f} I_{2\times 2}, \qquad A_{33} = \begin{bmatrix} -\frac{R_f}{L_f} & \omega_c \\ -\omega_c & -\frac{R_f}{L_f} \end{bmatrix},$$

$$B_3 = -\frac{v_{dc}}{2} A_{32}, \qquad A_{23} = -A_{21}.$$

It can be noted from (1) that the average model assumes that the PWM terminal voltage has only the fundamental component (v_s), and this fundamental component depends on the modulation index u_c (which is a control variable) and DC voltage. This is because the LC filter that comes after the PWM stage filters out most of the higher order harmonics and the voltage signal at the output terminal has mostly the fundamental component. However, the PWM terminal voltage is a stair-case signal with multiple harmonics. Even the magnitude of the fundamental component at the PWM terminal would be greater than at the output terminal considering the losses in the inverter side inductor of the filter.

B. Data Driven Model

An analytical expression that accurately represents v_s, is computationally tractable, and simple enough for control design is difficult to obtain. For this reason, this work uses a data driven approach to obtain such a model. Specifically, a block-oriented open-source neural network architecture, dynoNet [8], is chosen to identify the model.

By enabling long-term (or even infinite) time dependencies with a smaller number of parameters, dynoNet provides a clear advantage for system identification over traditional 1D convolutional neural networks. Furthermore, by leveraging linear recurrence equations in its LTI blocks, dynoNet can process time series data with less computational burden, along with providing the opportunity for parallelization as compared to traditional recurrent neural networks. The chosen Hamerstein-Weiner (HW) model structure, as seen in Fig. 3, is comprised of an input nonlinearity, followed by a linear system, followed by an output nonlinearity connected in series. The input and output nonlinearities are neural network based and can be further characterized by a combination of linear transformation layers and activation functions, such as $tanh$. By optimizing the weights and biases of the linear transformation layers embedded in the nonlinearity, along with the transfer function coefficients of the linear system, one can capture the nonlinear dynamics of the system while maintaining a linear-based model structure.

III. HW Model of the Test System

The test system shown in Fig. 1 is implemented in MATLAB/SIMULINK environment. The loads considered at the output of the inverter are linear in nature. The controller for the DC/DC converter has the objective of regulating the DC-link voltage to 600 V if there is sufficient solar irradiance. The details of this controller are not discussed as it is not the focus

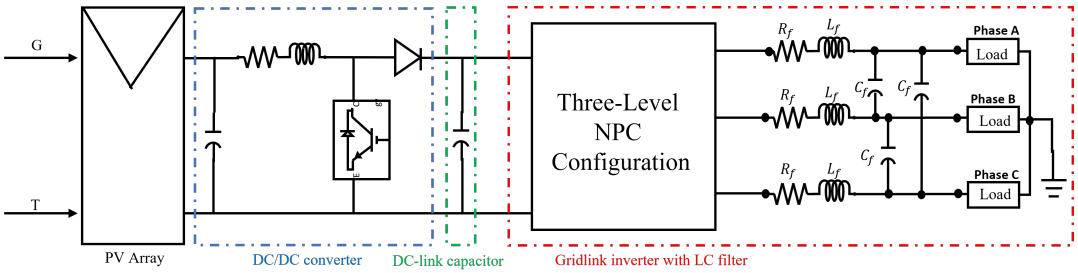

Fig. 1: Circuit Diagram of the test system

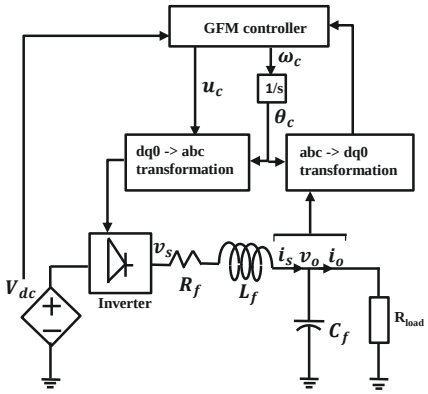

Fig. 2: Simplified single line diagram of the test system

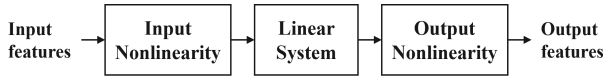

Fig. 3: Block Diagram of Hammerstein Weiner Model

of this paper. Similarly, during the training-data collection, the GFM controller is disabled, and the predefined input training features are used to collect the response of the test system. From the control design perspective, such an operation of the test system is known as open-loop operation as the control signal u_c does not depend on the feedback signals.

The data from open-loop GridLink inverter control responses were used to train the dynoNet HW model. The input features for the model are a) Control frequency (f_c), b) Direct axis (d) component of modulation index (u_d), c) Quadrature axis (q) component of modulation index (u_q), d) d component of output terminal voltage (v_{od}), and e) q component of output terminal voltage (v_{oq}). Similarly, the output features are a) DC-link voltage (V_{DC}), b) DC current (i_{DC}), c) d component of the output current (i_{od}), and d) q component of the output current (i_{oq}). After the data-set was obtained from the MATLAB/SIMULINK simulations, the training of the HW model was done in dynoNet platform using Python programming language. The details of the training are provided in Table I. The root mean square error (RMSE) values for the model training are [0.0019 0.0021 0.0017 0.0016] for I_d, I_{dc}, I_q, V_{dc}. The performance of the trained model for a validation data is provided in Fig. 4.

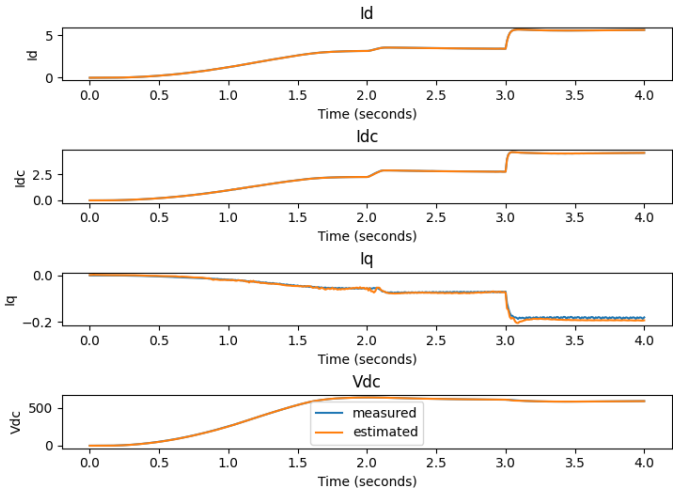

Fig. 4: Model Validation Case

TABLE I: dynoNet Modeling Parameters

Training Parameter	Value
TF Numerator Coefficients n_b	6
TF Denominator Coefficients n_a	6
Input Hidden Nodes	40
Output Hidden Nodes	30
Activation Function	tanh
Training Iterations	1000
Learning Rate	0.001

IV. Model Reference Controls of IBR

The standard approach for reference voltage tracking controller for a three-phase inverter is to design a proportional integral based cascaded control loop with an inner reference current tracking loop and the outer reference current generation loop [9]. Despite the popularity of this controller due to its simplicity, it has several limitations such as i) poor performance in unbalanced network conditions, and ii) requirement of anti-windup schemes to saturate and reset the action of the integrators in the outer loop during network fault conditions [10]. Alternatively, recursive feedback controller has been proposed in the literature [11], but they are model based controllers and assume that the average model of the inverter accurately represents the dynamics of the inverter. However, this is not true in reality as the average model leaves out the harmonic components present in the real hardware

circuit. As an improvement, model reference control (MRC) approach can be used which is the subject of discussion in this section.

MRC is a standard model-based feedback control framework [12]. As illustrated by Fig. 5(a), MRC calculates the tracking error between the reference model output and the plant output and uses it as the feedback control signal to design a dynamic feedback control under which the closed-loop input-output behavior of the plant matches that of the reference model. One can readily apply MRC to design IBR controls, as shown in Fig. 5(b). For instance, by choosing the reference model as

$$G_m(s) = \frac{1}{(s+\gamma_{vo})(s+\gamma_{is})}, \quad \gamma_{is}, \gamma_{vo} > 0,$$

the following GFM control has been developed in [11] to track the reference voltage (v_o^*):

$$u^* = -B_3^{-1}\left[A_{32}v_o + A_{33}i_s + \gamma_{is}(i_s - i_s^*) - \frac{di_s^*}{dt}\right] \quad (4)$$

$$i_s^* = -A_{23}^{-1}\left[A_{21}i_o + A_{22}v_o + \gamma_{vo}(v_o - v_o^*) - \frac{dv_o^*}{dt}\right] \quad (5)$$

where $\gamma_{vo}, \gamma_{is} > 0$ are control gains, and i_s^* is the reference current.

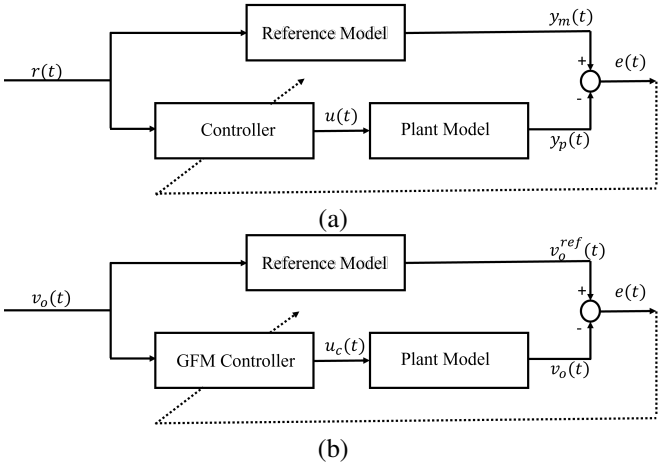

Fig. 5: MRC: (a) standard configuration; (b) IBR GFM control

The MRC framework is generally applicable to linear and nonlinear systems, but its drawback is that the plant model must be analytically known. In this paper, we aim to extend MRC by including a data-driven model and their corresponding control design, as described in the following two subsections.

A. MRC for IBRs with a Data-Driven EMT Model

PWM controlled inverters do inherently have electromagnetic transients (EMTs) that are not captured by their average dynamic model. Using the proposed HW model, one can model inverter dynamics including EMT to an accuracy of 98% or better. This means that a data-driven model of EMT is obtained. Specifically, the inverter dynamics (Fig. 6(a)) is captured by its HW model (Fig. 6(b)) and, since the IBR output can be decomposed into standard non-switching (i.e. ideal) RMS response described by the average model and an additive EMT response as shown in Fig. 6(c), the data-driven EMT model is found to be that depicted in Fig. 6(d).

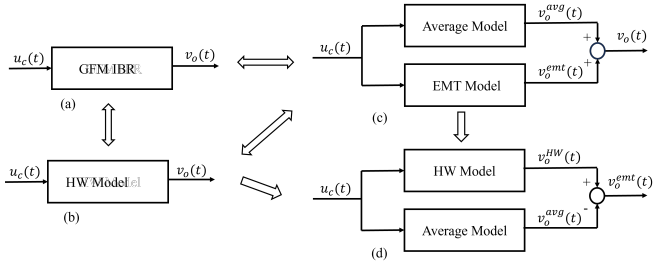

Fig. 6: Inverter EMT Modeling: (a) inverter; (b) HW model; (c) EMT decomposition; (d) EMT model

Upon having the data-driven EMT model, the MRC framework can be applied to compensate for EMT, as illustrated in Fig. 7. The control structure in Fig. 7 consists of two concatenated MRC loops: the outer loop is the same as that in Fig. 5(b), while the inner loop is the EMT control loop. There is no reference model explicitly given for the inner loop because it is zero (in the sense that removal of EMT is the control objective).

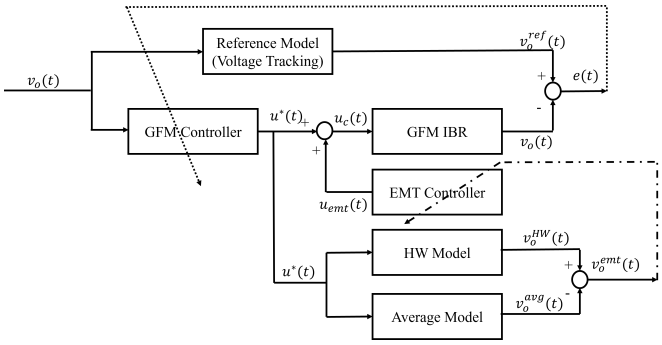

Fig. 7: Model reference control for compensating for EMT

In the next subsection, the EMT compensation control is explicitly developed and synthesized.

B. MRC Design to Compensate for EMT

As shown in Fig. 6, we know that, around the nominal operating voltage v_o^* and under any control input v_s,

$$v_o = v_o^{avg} + v_o^{emt}. \quad (6)$$

Our objective is to design the following MRC:

$$u_c = u^* + u_{emt}, \quad (7)$$

where u^* is the nominal GFM control under which v_o^{avg} converges to v_o^*. The incremental control u_{emt} is to be designed to remove v_o^{emt} from v_o (to the extent possible).

It follows from (1), (2), and (3) that

$$v_o^{avg} = G_v(s)v_s^{avg} + G_f(s)i_o = G_v(s)v_s^{avg} + \frac{1}{Z(s)}G_f(s)v_o^{avg},$$

or simply

$$v_o^{avg} = G(s)v_s^{avg} = \frac{V_{dc}}{2}G(s)u_c, \quad G(s) = \frac{G_v(s)Z(s)}{Z(s) - G_f(s)}, \tag{8}$$

where $Z(s)$ is the equivalent impedance of the grid, and the transfer functions $G_v(s)$ and $G_f(s)$ are defined as

$$G_v(s) = H(sI - F)^{-1}G, \quad G_f(s) = (sI - F)^{-1}E \tag{9}$$

$$F = \begin{bmatrix} A_{22} & A_{23} \\ A_{32} & A_{33} \end{bmatrix}, \quad G = \frac{1}{L_f}\begin{bmatrix} 0_{2\times 2} \\ I_{2\times 2} \end{bmatrix},$$

$$H = \begin{bmatrix} I_{2\times 2} & 0_{2\times 2} \end{bmatrix}, \quad E = -\frac{1}{C_f}H^T.$$

Since the HW model has been trained to represent the actual inverter system, we know from Fig. 7 that, under input $u^*(t)$, the HW model predicts well the output voltage of the inverter as

$$\begin{aligned} v_o^{HW} &\simeq v_o \\ &= v_o^{avg}\big|_{u=u^*} + v_o^{emt}\big|_{u=u^*} \\ &= v_o^* + v_o^{emt}\big|_{u=u^*}, \end{aligned}$$

or simply,

$$v_o^{emt}\big|_{u=u^*} \simeq v_o^{HW} - v_o^*. \tag{10}$$

It follows from (6) and (8) that, under MRC (7),

$$\begin{aligned} v_o\big|_{u=u^*+u_{emt}} &= v_o^{avg}\big|_{u=u^*+u_{emt}} + v_o^{emt}\big|_{u=u^*+u_{emt}} \\ &= \frac{V_{dc}}{2}G(s)(u^* + u_{emt}) + v_o^{emt}\big|_{u=u^*+u_{emt}} \\ &= v_o^* + \frac{V_{dc}}{2}G(s)u_{emt} + v_o^{emt}\big|_{u=u^*+u_{emt}} \\ &\simeq v_o^* + \frac{V_{dc}}{2}G(s)u_{emt} + v_o^{emt}\big|_{u=u^*} \\ &\simeq \frac{V_{dc}}{2}G(s)u_{emt} + v_o^{HW}, \end{aligned}$$

in which (10) is applied and the following approximation is made:

$$v_o^{emt}\big|_{u=u^*+u_{emt}} \simeq v_o^{emt}\big|_{u=u^*}$$

because v_{emt} is much smaller compared to v_o^* and, due to u_{emt} being much smaller than u^*, the EMT incremental change is neglectable. Given the control objective of making $v_o\big|_{u=u^*+u_{emt}}$ converge to output component v_o^{avg} (that is, zeroing out v_o^{emt}), we can choose the following feedback control:

$$u_{emt} = -k_1\hat{G}^{-1}(s)\frac{2}{V_{dc}}\left[v_o^{HW} - k_2 v_o^{avg}\right] \tag{11}$$

$$= -k_1\left[v_s^{HW} - k_2 v_s^{avg}\right], \tag{12}$$

where k_1 and k_2 are positive control gains, and $\hat{G}^{-1}(s)$ is any causal inverse of transfer function $G(s)$. Expressions (11) and (12) are mathematically equivalent but, for implementation, control (12) is simpler as it does not require information about the grid while v_s^{HW} and v_s^{avg} can be either measured or estimated.

V. Results and Discussions

The test system in Fig. 1 is implemented in MATLAB/SIMULINK, with a three-level neutral-point-clamped (NPC) inverter. In this implementation and the corresponding hardware demonstration, dead bands are used in the PWM scheme to separate the operation of complementary switches in the same leg. These nonlinear effects are absent in the average model implementation, but they together with PMW switchings contribute to EMT. In addition, the proposed HW model trained in dynoNet and the average model are also implemented using MATLAB/SIMULINK.

The following MRC with specific gain choices is implemented:

$$u_{emt} = -\frac{u_d^*}{v_{s,d}^{HW}}\left[v_s^{HW} - k_2 v_s^{avg}\right], \tag{13}$$

where $k_2 = 1$ is the nominal value but can be fine tuned further. Feedback v_s^{avg} is obtained from (1), and v_s^{HW} is estimated by feeding v_o^{HW} through the inverse of LC filter's transfer function. The voltage tracking results and the EMT compensation results are presented in Fig. 8 and Fig. 9 respectively. The entire test duration consists of the following three segments:

- t $\in [0,\ 1.1)$ second: the solar irradiance ramps up from 0 W/M^2 to $1000W/M^2$. The GFM control is disabled, and the test system is excited with an open loop control signal $u_c = [1; 0.001; 0]$. This step is carried out in order to let the trained HW model initialize properly as it has been trained in the similar manner. Fig. 8 shows a spike in the response of this HW model implementation in MATLAB at $t = 0$s, after which it responds accurately. Better initialization procedures are available [7], but were not necessary for this application.
- t $\in [1.1,\ 4)$: the open loop control signal is changed to $u_c = [1; 0.001; 0]$. This is done to check how the HW model would behave once the irradiation reaches the steady state. It can be observed from Fig. 8 that the HW model is responding more accurately compared to average model.
- t $\in [4,\ 8.5)$: the nominal GFM control is activated. It can be observed from Fig. 8 that the inverter is able to track the reference voltage with a high degree of accuracy even though the average model assumed for the inverter control design does not hold true. This shows that the nominal GFM control designed is already a robust controller. In addition, the perfect voltage tracking would be observed (i.e., the green curves) should the assumption of average model would hold true, and this result also reveals that the performance of the GFM controller could be improved further by accounting for modeling inaccuracies. Upon applying the proposed MRC, it can be observed from Fig. 9 that the EMT components of the output voltage are substantially reduced.
- t $\in [8.5,\ 12]$: the MRC is tuned to one with $k_2 = 1.08$ in (13). It can be observed from Fig. 8 that the inverter is able to accurately track the reference voltage. The slight

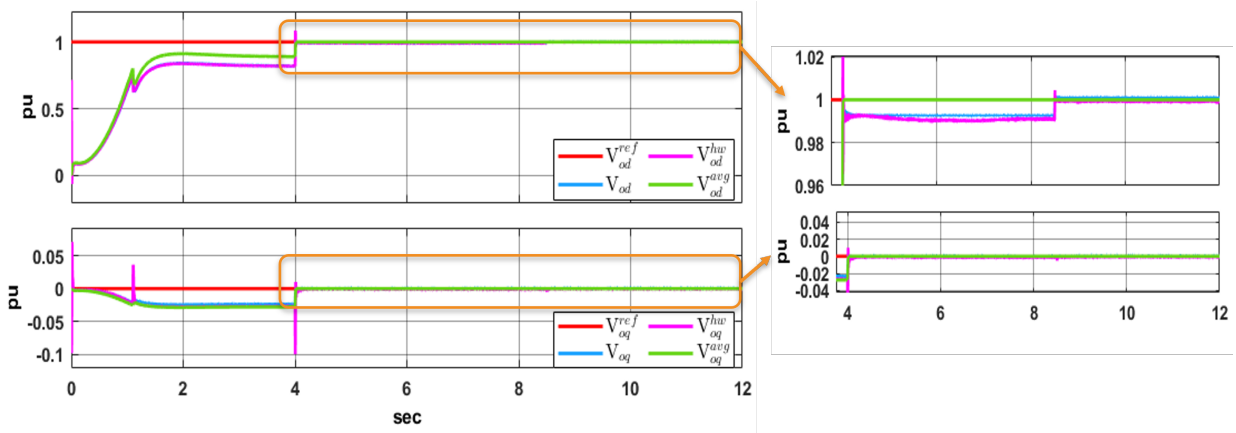

Fig. 8: Voltage tracking using model reference control approach

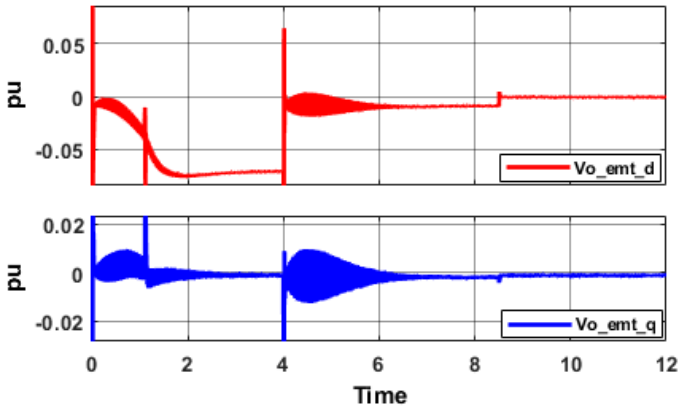

Fig. 9: EMT compensation using MRC approach

deviation of k_2 from one is because the MRC itself has an effect on EMT, which is not captured by the HW model since u^* is used with the HW model as shown in Fig. 7. And, this tuning further reduces the EMT components, as shown in Fig. 9.

VI. Conclusion

In this paper, a nonlinear data-driven model is proposed for grid operation of three-phase inverter based resources (IBRs). The proposed model is a Hammerstein Wiener (HW) model whose parameters can be easily trained using open-source deep-learning platform, *dynoNet*. The proposed model can accurately capture the EMT dynamics present in the detailed switching model of the inverter, and it is computationally comparable to any continuous-time nonlinear dynamic model and hence adequate for real-time control implementation. As an application of the HW model, a MRC is developed for three-phase IBRs to perform reference voltage tracking and also compensate for their own EMT. Our high-fidelity results show that the proposed MRC is very effective in both grid forming functionality and EMT compensation.

References

[1] Solar Energy Technologies Office, "Solar integration: Inverters and grid services basics." [Online]. Available: https://www.energy.gov/eere/solar/solar-integration-inverters-and-grid-services-basics

[2] A. M. Gole, A. Keri, C. Nwankpa, E. W. Gunther, H. W. Dommel, I. Hassan, J. R. Marti, J. A. Martinez, K. G. Fehrle, L. Tang, M. F. McGranaghan, O. B. Nayak, P. F. Ribeiro, R. Iravani, and R. Lasseter, "Guidelines for modeling power electronics in electric power engineering applications," *IEEE Transactions on Power Delivery*, vol. 12, no. 1, p. 505, January 1997.

[3] V. Vorperian, R. Tymerski, and F. C. Y. Lee, "Equivalent circuit models for resonant and pwm switches," *IEEE Transactions on Power Electronics*, vol. 4, no. 2, pp. 205–212, April 1989.

[4] N. Guruwacharya, N. Bhujel, U. Tamrakar, M. Rauniyar, S. Subedi, S. E. Berg, T. M. Hansen, and R. Tonkoski, "Data-driven power electronic converter modeling for low inertia power system dynamic studies," in *2020 IEEE Power & Energy Society General Meeting*, 2020, pp. 1–5.

[5] N. Guruwacharya, H. Bhandari, S. Subedi, J. D. Vasquez-Plaza, M. L. Stoel, U. Tamrakar, F. Wilches-Bernal, F. Andrade, T. M. Hansen, and R. Tonkoski, "Data-driven modeling of commercial photovoltaic inverter dynamics using power hardware-in-the-loop," in *2022 International Symposium on Power Electronics, Electrical Drives, Automation and Motion (SPEEDAM)*, 2022, pp. 924–929.

[6] N. Patcharaprakiti, K. Kirtikara, V. Monyakul, D. Chenvidhya, J. Thongpron, A. Sangswang, and B. Muenpinij, "Modeling of single phase inverter of photovoltaic system using hammerstein–wiener nonlinear system identification," *Current Applied Physics*, vol. 10, no. 3, Supplement, pp. S532–S536, 2010.

[7] T. E. McDermott, Q. Huang, Y. Liu, D. Glover, M. Ramesh, K. McDonald, G. Marasini, and Z. Qu, "Deep learning-enhanced block diagram modeling of solar power systems," 2024, accepted to present in 2024 IEEE eGrid Workshop.

[8] M. Forgione and D. Piga, "*dynoNet*: A neural network architecture for learning dynamical systems," *International Journal of Adaptive Control and Signal Processing*, vol. 35, no. 4, pp. 612–626, 2021.

[9] A. Sangwongwanich, A. Abdelhakim, Y. Yang, and K. Zhou, "Control of single-phase and three-phase dc/ac converters," in *Control of Power Electronic Converters and Systems*. Academic Press, 2018, pp. 153–173.

[10] B. Fan, T. Liu, F. Zhao, H. Wu, and X. Wang, "A review of current-limiting control of grid-forming inverters under symmetrical disturbances," *IEEE Open Journal of Power Electronics*, vol. 3, pp. 955–969, 2022.

[11] S. Nag, Z. Qu, and Y. Xu, "A unified grid-forming and grid-following primary control design with optimized enforcement of grid operational constraints," *IEEE Access*, vol. 11, pp. 57 415–57 427, 2023.

[12] H. Butler, *Model Reference Adaptive Control: From Theory to Practice*. Prentice Hall, 1992.